Improving the Drift Effect and Hysteresis Effect of Urea Biosensor Based on Graphene Oxide/Nickel Oxide Sensing Film Modified Either by Au Nanoparticles or γ-Fe$_2$O$_3$ Nanoparticles Using Back-End Calibration Circuit

YU-HSUN NIEN [1] (Member, IEEE), TZU-YU SU[1], JUNG-CHUAN CHOU [2] (Senior Member, IEEE),
PO-YU KUO [2] (Member, IEEE), CHIH-HSIEN LAI [2] (Member, IEEE), CHIH-SUNG HO [3],
ZHE-XIN DONG [2] (Member, IEEE), ZHI-XUAN KANG[1], AND TSU-YANG LAI[2]

1 Graduate School of Chemical and Materials Engineering, National Yunlin University of Science and Technology, Douliou 64002, Taiwan
2 Graduate School of Electronic Engineering, National Yunlin University of Science and Technology, Douliou 64002, Taiwan
3 Graduate School of Department of Chemical and Materials Engineering, Tunghai University, Taichung 407302, Taiwan

CORRESPONDING AUTHOR: J.-C. CHOU (e-mail: choujc@yuntech.edu.tw)

ABSTRACT From our other works, we have developed urea biosensor based on graphene oxide/nickel oxide sensing film modified either by Au nanoparticles or γ-Fe$_2$O$_3$ nanoparticles. In this study, we have further developed back-end calibration circuit to reduce the drift effect and hysteresis effect of the two types of the urea biosensors. The back-end calibration circuit is composed of non-inverting amplifiers, error amplifiers, P-MOSFET transmission transistor, feedback networks, output voltage capacitors and resistor dividers. After applying the back-end calibration circuit, the drift rate of urea biosensor modified by Au NPs is reduced from 3.06 mV/hr to 0.28 mV/hr, which is 90.85% reduction. The drift rate of urea biosensor modified by γ-Fe$_2$O$_3$ NPs is reduced from 3.92 mV/hr to 0.57 mV/hr, which is 85.46% reduction. Through the back-end calibration circuit to reduce the hysteresis effect, the hysteresis voltage for the forward cycle and reverse cycle of the urea biosensor modified by Au NPs are reduced by 26% and 30%, respectively. The hysteresis voltage for the forward cycle and reverse cycle of the urea biosensor modified by γ-Fe$_2$O$_3$ NPs are reduced by 23% and 28%, respectively.

INDEX TERMS Au nanoparticles (Au NPs), flexible substrate, graphene oxide (GO), maghemite nanoparticles (γ-Fe$_2$O$_3$ NPs), nickel oxide (NiO), urea biosensor, urease.

I. INTRODUCTION

Urea is the final product during the metabolism of protein in the human body, and its level ranges from 2.5 to 7.5 mM [1]. Abnormal changes in urea level may indicate diseases in the kidney or liver, such as kidney failure or liver failure, etc, [2]. There are many techniques for the determination of urea, such as colorimetry [3], fluorimetry [4], spectrophotometry [5], HPLC [6], chemiluminometric [7], etc. However, the disadvantages of these methods are time-consuming for sample preparation, high-cost in equipment, necessary to operate by skilled operators and not suitable for on-site testing. Recently, the electrochemical based methods overcome the above disadvantages, and have the advantages of low manufacturing cost, high sensitivity and high selectivity [8], [9]. There are many techniques for the electrochemical, such as metal ion-induced optical [10], fluorescence detection [11]. They are considered to be better alternatives for urea determination.

Nanomaterials possess several properties such as high surface area/volume ratio, excellent electron conductivity [12], electrocatalytic performance [13] and suitable matrix for enzyme immobilization [14], which can improve the performance of biosensors. They are documented as one of the most attractive materials in the development of next-generation biosensors [15]. From our other works, we have developed urea biosensor based on graphene oxide/nickel oxide sensing films modified either by Au nanoparticles or γ-Fe$_2$O$_3$ nanoparticles [16], [17]. Due to the high chemical stability, high catalytic activity, simple synthesis method and good biocompatibility of Au NPs, they provide excellent sensing characteristics for urea biosensor [16], [18]. The γ-Fe$_2$O$_3$ NPs have excellent electron transfer performance, effective surface area and low cost, and are one of the promising materials for electrochemical biosensors [17], [18].

The sensitivity, response time and detection limit of urea biosensors have been widely studied. However, few researchers have studied the drift effect of urea biosensors. The drift behavior is due to the increase in the thickness of the hydrated layer during the long-term measurement, which leads to an increase in the drift rate [19]. In this article, we further apply back-end calibration circuit, which is developed by Kuo and Dong [20] to reduce the drift effect and hysteresis effect of the two types of the urea biosensors.

II. EXPERIMENTAL
A. MATERIALS
Polyethylene terephthalate (PET) was used as the substrate of the biosensor and it was purchased from Zencatec Corp., (Taiwan). Silver conductive paste was procured from Advanced Electronic Material Inc., (Taiwan). Nickel oxide (NiO) target with 99.95% purity was bought from Ultimate Materials Technology Corp., Ltd. (Taiwan). Graphite powder was obtained from Alfa Aesar, (USA). Sodium nitrate (NaNO$_3$) was supplied from Sigma-Aldrich Corp., (USA). Hydrochloric acid (HCl) and sulfuric acid (H$_2$SO$_4$) were procured from Nihon Shiyak Industries Ltd., (Japan). Hydrogen peroxide (H$_2$O$_2$) was bought from Choneye Pure Chemical, (Taiwan). Tetrachloroauric (III) acid trihydrate (HAuCl$_4$ · 3H_2O) was purchased from Acros Organics, (Belgium). Tri-sodium citrate 2-hydrate (Na$_3$C$_6$H$_5$O$_7$ · 2H_2O) was acquired from Acros Organics, (USA). Iron (0) pentacarbonyl (Fe(CO)$_5$), dioctyl ether, oleic acid, α-cyclodextrin, and urease was purchased from Sigma-Aldrich Corp., (USA). Urea powder was gained from J. T. baker Corp., (USA).

B. THE SYNTHESIS OF AU NPS AND γ-FE$_2$O$_3$ NPS
The synthesis processes of the Au NPs solution were as follows:
1) 5 mM of chloroauric acid (HAuCl$_4$ · 3H_2O) solution was added to 40 mL of D.I. water and heating at 100 °C.
2) 1 g of sodium citrate (Na$_3$C$_6$H$_5$O$_7$ · 2H_2O) was dissolved in D.I. water.

3) 5 mL of the sodium citrate solution was added to step (1).
4) When the mixed solution changed color, turn off the heating and the Au NPs were completed.

The synthesis processes of the γ-Fe$_2$O$_3$ NPs solution were as follows:
1) 0.96 mL of oleic acid and 10 mL of octyl ether were mixed in florence flask and heated to 100 °C.
2) Fe(CO)$_5$ was quickly added to step (1) and heated to 295 °C.
3) When the mixed solution changed color, the synthesis of γ-Fe$_2$O$_3$ NPs were completed.

The γ-Fe$_2$O$_3$ NPs were not soluble in water. Hence, the γ-Fe$_2$O$_3$ NPs were modified from oil-soluble to water-soluble.
1) The oil-soluble γ-Fe$_2$O$_3$ NPs were dispersed in n-hexane solvent.
2) α-cyclodextrin solution was added to step (1) and stirred for 35 hr.
3) After the reaction, the water-soluble γ-Fe$_2$O$_3$ NPs were completed.

C. THE FABRICATION OF UREA BIOSENSOR MODIFIED BY AU NPS AND γ-FE$_2$O$_3$ NPS
The fabrication of the urea biosensor is based on previous research.
1) Conductive wire and reference electrodes were integrated on the PET substrate by screen printing technology.
2) Epoxy was used to define the sensing window by screen printing technology.
3) 0.3 wt% GO solution was dropped on the NiO sensing film, which was the optimal parameter.
4) 2 µl of γ-APTS and 2 µl of glutaraldehyde were dropped on the GO/NiO sensing film, respectively, which could enhance the adsorption ability of urease.
5) Either Au NPs solution (5mM) or γ-Fe$_2$O$_3$ NPs solution (1mg/ml) was mixed with urease solution (10mg/ul), respectively.

Either urease-Au NPs mixed solution or urease-γ-Fe$_2$O$_3$ NPs mixed solution was dropped on the GO/NiO sensing film, respectively. The urea biosensors were completed. The structure of urea biosensor is shown in Fig. 1.

D. THE VOLTAGE-TIME (V-T) MEASUREMENT SYSTEM
The V-T measurement system has been reported in previous researches [19], [21], [22]. It is shown in Fig. 2, which is composed of LT1167, DAQ Card, and LabVIEW software. The LT1167 is an instrumentation amplifier. The DAQ Card is a data acquisition card. After the input voltage difference of the working electrode and the reference electrode is amplified by the LT1167, and the data are transmitted to acquisition card to convert the analog signal into a digital signal, then the data is analyzed by LabVIEW software. The formula of output voltage of LT1167 is as follows:

$$V_{out} = V_{in1} - V_{in2} = V_{ref} - V_{work} = -V_{work} \qquad (1)$$
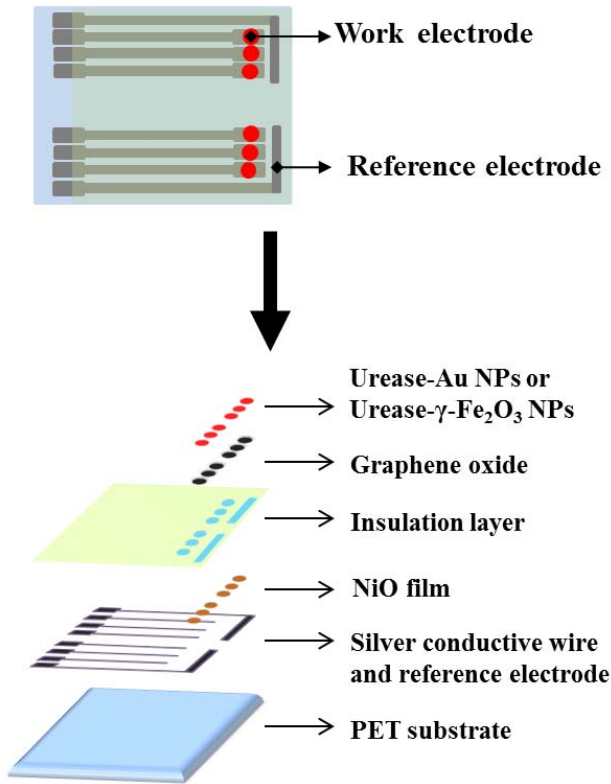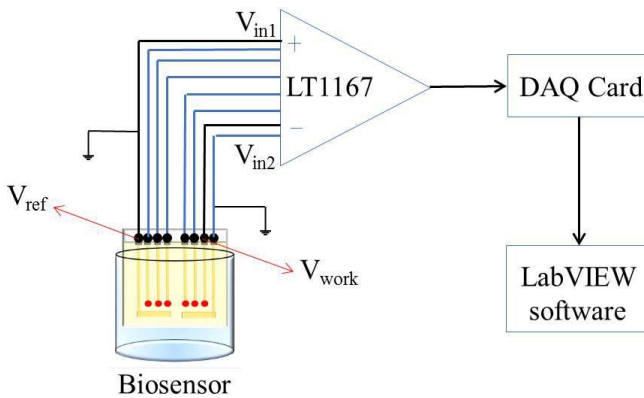
FIGURE 1. The structure of urea biosensor.

FIGURE 2. The structure diagram of V-T measurement system.

where V_{out} is the output voltage of the LT1167, V_{in1} is the positive input of the LT1167, V_{in2} is the negative input of the LT1167, V_{ref} is the voltage of the reference electrode, and V_{work} is the voltage of the working electrode.

E. THE BACK-END CALIBRATION CIRCUIT

The back-end calibration circuit is composed of non-inverting amplifiers (A_1, R_1 and R_2), error amplifiers (A_2), P-MOSFET transmission transistor (M_p), feedback networks (R_3 and R_4), output voltage capacitors (C_{out}) and resistor dividers (R_5 and R_6).

The magnification of the amplifier is controlled in unsaturated mode. The response voltage of the biosensor is
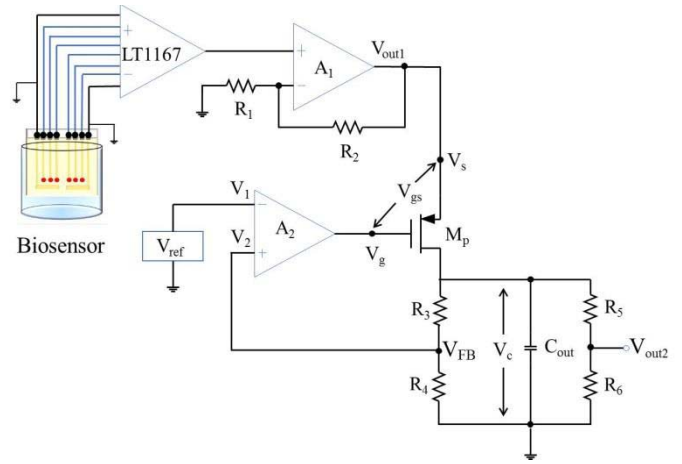

FIGURE 3. The structure diagram of back-end calibration circuit [20].

amplified by the non-inverting amplifier, so that the M_p can be transmitted in the linear region. M_p can provide the output current to charge the C_{out}, thereby maintaining V_c at a certain level. The mechanism of voltage regulation is implemented by negative feedback networks (R_3 and R_4), which is expressed by formula (2).

$$V_{FB} = V_c \times \frac{R_4}{R_3 + R_4} \qquad (2)$$

According to formula (2), when the output voltage of V_c decreases, V_{FB} decreases, resulting in a decrease in the output voltage of A_2. As the output voltage of A_2 decreases, the gate voltage of M_p also decreases. Therefore, the gate-source voltage (V_{gs}) of M_p increases and generate more current to charge the output capacitor so that the output voltage of V_c can maintain at a certain level. On the contrary, by changing the voltage and current, the output voltage is maintained at the certain level in a short time [20].

The response voltages of the biosensor is amplified by the non-inverting amplifier and input into the back-end calibration circuit. In order to obtain the original response voltage of the biosensor, the original amplification factor is reduced by a voltage divider (R_5 and R_6). The output voltage (V_{out2}) is calculated using formula (3). The schematic diagram of the back-end calibration circuit to reduce drift effect is shown in Fig. 3.

$$V_{out2} = V_c \times \frac{R_6}{R_5 + R_6}. \qquad (3)$$

III. RESULTS AND DISCUSSION
A. THE AVERAGE SENSITIVITY AND LINEARITY OF UREA BIOSENSOR BY V-T MEASUREMENT SYSTEM

The basic sensing mechanism of the urea biosensor was based on the enzymatic reaction catalyzed by urease.

$$NH_2CONH_2 + 3H_2O\ 2NH_4^+ + HCO_3^- + OH^- \qquad (4)$$
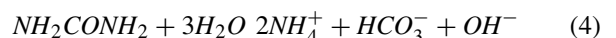
According to formula (4), ammonium (NH_4^+), bicarbonate (HCO_3^-) and hydroxide ion (OH^-) are the products
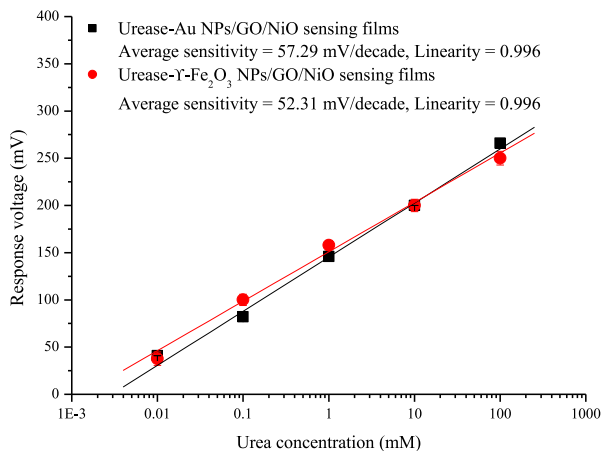
FIGURE 4. The average sensitivities and linearities of urea biosensors based on different sensing film.

TABLE 1. The average sensitivities and linearities of urea biosensor based on different sensing films.

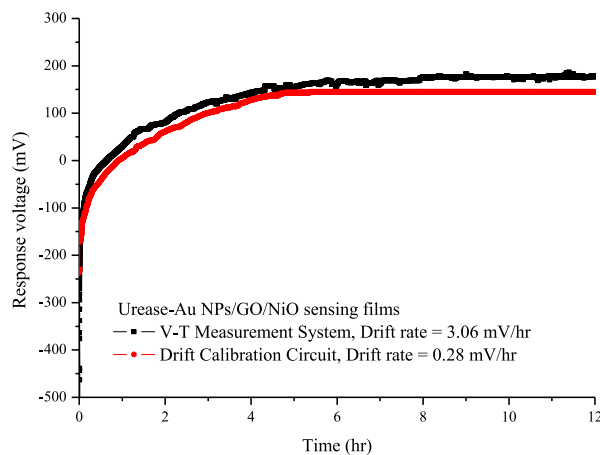| Sensing film	Average sensitivity ± SD (mV/decade)	Linearity
NiO	32.02±0.19	0.995
GO/NiO	40.29±0.42	0.996
Urease-Au NPs/GO/NiO	57.07±0.72	0.996
Urease-γ-Fe$_2$O$_3$ NPs/GO/NiO	52.03±0.38	0.996

FIGURE 5. The drift effect of the urea biosensor based on urease-Au NPs/GO/NiO sensing film measured by V-T measurement system and back-end calibration circuit, respectively.

of urea catalyzed by urease. In this reaction, the hydroxide ions are directly generated onto the surface of sensing windows. An increase in hydroxide ions concentration produces a potential change on the electrode surface, which is proportional to the urea concentration [23]–[25].

Five urea biosensors were manufactured for each type of the biosensors and their performances were evaluated. Each biosensor contained six sensing windows. Five different concentrations of test solutions were measured under the same environmental conditions, and the measurement time for each test solution was 30 s. The sensitivity of NiO sensing film and GO/NiO sensing film were 32.02±0.19 mV/decade and 40.29±0.42 mV/decade, respectively. After GO/NiO sensing film modified either by Au NPs or γ-Fe$_2$O$_3$ NPs, the sensitivity was increased to 57.07±0.72 mV/decade and 52.03±0.38 mV/decade, respectively.

Because either Au NPs or γ-Fe$_2$O$_3$ NPs is nanomaterials with excellent electronic conductivity, and can also be used as an excellent substrate for immobilized enzymes, thereby improving the performance of biosensors [16]–[18]. The average sensitivities and linearities of urea biosensors modified either by Au NPs or γ-Fe$_2$O$_3$ NPs are shown in Fig. 4 and Table 1.

B. THE DRIFT EFFECT OF UREA BIOSENSOR BY VOLTAGE-TIME (V-T) MEASUREMENT SYSTEM AND BACK-END CALIBRATION CIRCUIT

The drift is defined as the monotonic change of response in accordance with the measured time, which is a non-ideal effect [26]. The formation of drift behavior is that OH^- ions increase the thickness of the hydrated layer under the long-term measured duration leading to the increase of drift rate. The drift rate is the response voltage per hour between the 5th and the 12th hour. The formula is as follows:

$$\text{Drift rate} = \frac{V_{12\text{th}} - V_{5\text{th}}}{t} \quad (5)$$

where $V_{12\text{th}}$ is the response voltage in the 12th hr, $V_{5\text{th}}$ is the response voltage in the 5th hr and t is the measurement time.

In this work, the urea biosensor was immersed in the PBS solution with 5 mM of urea concentration and measured for 12 hr by both V-T measurement system and back-end calibration circuit, respectively. According to the experimental results, the drift rates of the urea biosensor modified by Au NPs were 3.06 mV/hr and 0.28 mV/hr measured by the V-T measurement system and back-end calibration circuit, respectively. As shown in Fig. 5, through the measurement of the back-end calibration circuit, the drift rate of the urea biosensor modified by Au NPs could be reduced by 90.85%.

The drift rates of the urea biosensor modified by γ-Fe$_2$O$_3$ NPs were 3.92 mV/hr and 0.57 mV/hr measured by the V-T measurement system and back-end calibration circuit, respectively. As shown in Fig. 6, through the measurement of the back-end calibration circuit, the drift rate of the urea biosensor modified by γ-Fe$_2$O$_3$ NPs could be reduced by 85.46%.

This experiment is repeated seven times and the results are shown in Table 2.

C. THE HYSTERESIS EFFECT OF UREA BIOSENSOR BY VOLTAGE-TIME (V-T) MEASUREMENT SYSTEM AND BACK-END CALIBRATION CIRCUIT

The hysteresis effect is another non-ideal effect in repeated measurements of sensors. According to the report by
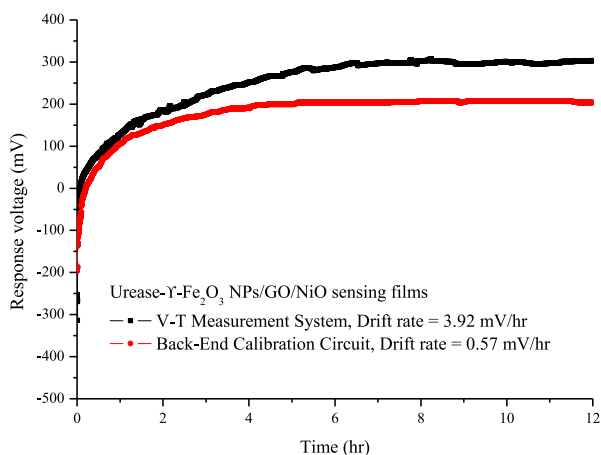
FIGURE 6. The drift effect of the urea biosensor based on urease-γ-Fe$_2$O$_3$ NPs/GO/NiO sensing film measured by V-T measurement system and back-end calibration circuit, respectively.

TABLE 2. The drift effect of urea biosensor based on different sensing films.

Structure	Number of Sensors	by V-T Measurement System	by Back-End Calibration Circuit
urease-Au NPs/GO/NiO sensing film	1	3.06 mV/hr	0.28 mV/hr
	2	3.21 mV/hr	0.51 mV/hr
	3	3.08 mV/hr	0.31 mV/hr
	4	3.11 mV/hr	0.39 mV/hr
	5	3.15 mV/hr	0.45 mV/hr
	6	3.19 mV/hr	0.49 mV/hr
	7	3.25 mV/hr	0.53 mV/hr
urease-γ-Fe$_2$O$_3$ NPs/GO/NiO sensing film	1	3.92 mV/hr	0.57 mV/hr
	2	3.99 mV/hr	0.65 mV/hr
	3	4.01 mV/hr	0.68 mV/hr
	4	4.25 mV/hr	0.94 mV/hr
	5	4.09 mV/hr	0.79 mV/hr
	6	4.16 mV/hr	0.85 mV/hr
	7	4.22 mV/hr	0.92 mV/hr

Bousse *et al.* the hysteresis effect of pH-ISFET can be regarded as a delay in pH response [27]. The hysteresis effect of urea biosensor can be also regarded as the delay of the concentration response.

In this work, we evaluated the stability and the reversibility of the potentiometric flexible arrayed urea biosensor for hysteresis effect by V-T measurement system and back-end calibration circuit. The urea biosensor was immersed in the PBS solution with urea for measured in forward cycle and reverse cycle by V-T measurement system. The immersion was in the order of 5mM $\rightarrow$ 1.66mM $\rightarrow$ 5mM $\rightarrow$ 8.33mM $\rightarrow$ 5mM (forward cycle) and 5mM $\rightarrow$ 8.33mM $\rightarrow$ 5mM $\rightarrow$ 1.66mM $\rightarrow$ 5mM (reverse cycle). The hysteresis voltage (V_H) was the difference between the initial voltage and the final voltage [28].

The potentiometric flexible arrayed urea biosensor based on GO/NiO sensing film modified by Au NPs was measured
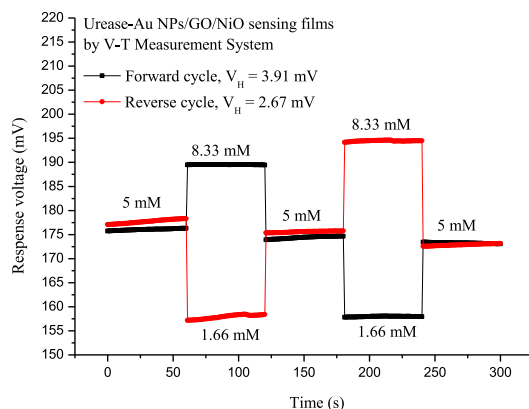

FIGURE 7. The hysteresis effect of the urea biosensor based on urease-Au NPs/GO/NiO sensing films measured by V-T measurement system.
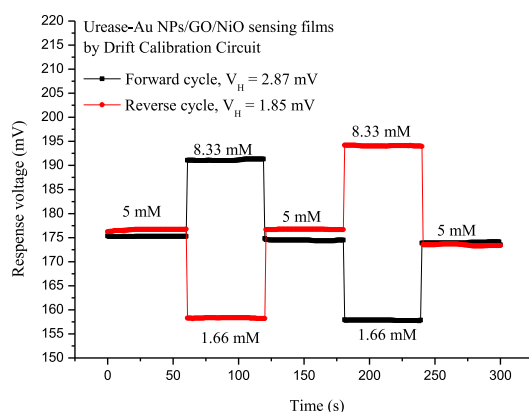

FIGURE 8. The hysteresis effect of the urea biosensor based on urease-Au NPs/GO/NiO sensing film measured by back-end calibration circuit.

by V-T measurement system. According to the experimental results, the V_H were 3.91 mV and 2.67 mV for the forward cycle and reverse cycle, respectively, as shown in Fig. 9. Due to the size of H$^+$ ions was smaller than that of OH$^-$ ions, which indicated that the diffusion rate of H$^+$ ions was faster than that of OH$^-$ ions. Because of this difference, the hysteresis voltage was generated [29].

The potentiometric flexible arrayed urea biosensor based on GO/NiO sensing film modified by Au NPs was measured by back-end calibration circuit. According to the experimental results, the V_H were 2.87 mV and 1.85 mV in the forward cycle and reverse cycle, respectively, as shown in Fig. 7. Through the back-end calibration circuit, the V_H for the forward cycle and reverse cycle of the potentiometric flexible arrayed urea biosensor based on GO/NiO sensing film modified by Au NPs were reduced by 26% and 30%, respectively, as shown in Fig. 8.

The potentiometric flexible arrayed urea biosensor based on GO/NiO sensing film modified by γ-Fe$_2$O$_3$ NPs was measured by V-T measurement system. According to the experimental results, the V_H were 5.07 mV and 4.27 mV for the forward cycle and reverse cycle, respectively, as shown in Fig. 9. Through the back-end calibration circuit, the V_H
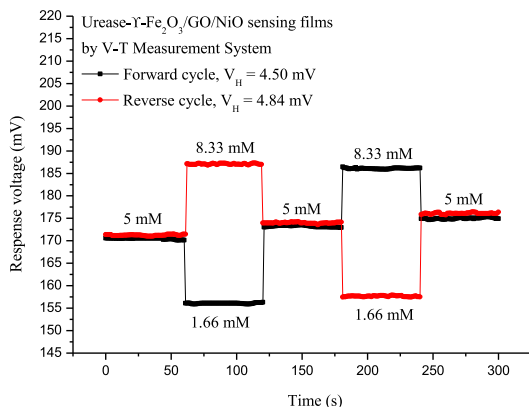
FIGURE 9. The hysteresis effect of the urea biosensor based on urease-γ-Fe$_2$O$_3$ NPs/GO/NiO sensing film measured by V-T measurement system.
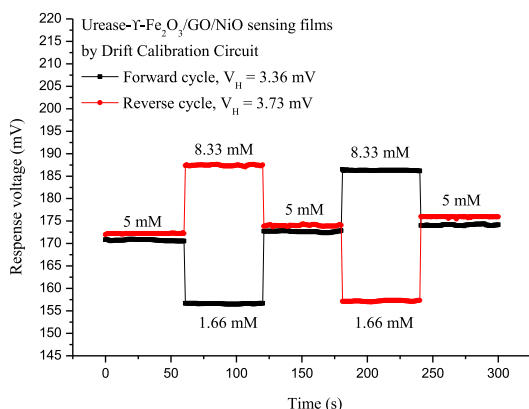

FIGURE 10. The hysteresis effect of the urea biosensor based on urease-γ-Fe$_2$O$_3$ NPs/GO/NiO sensing film measured by back-end calibration circuit.

for the forward cycle and reverse cycle were 3.89 mV and 3.05 mV, respectively. The reductions were 23% and 28%, respectively, as shown in Fig. 10.

IV. CONCLUSION

In this work, we have fabricated the urea biosensor modified either by Au NPs or γ-Fe$_2$O$_3$ NPs. The average sensitivity and linearity of the urea biosensor modified by Au NPs were 57.07±0.72 mV/decade and 0.996, respectively. The average sensitivity and linearity of the urea biosensor modified by γ-Fe$_2$O$_3$ NPs were 52.03±0.38 mV/decade and 0.996, respectively. After applying the back-end calibration circuit, the drift rate of the urea biosensor modified by Au NPs was reduced from 3.06 mV/hr to 0.28 mV/hr, which was 90.85% reduction. The drift rate of the urea biosensor modified by γ-Fe$_2$O$_3$ NPs was reduced from 3.92 mV/hr to 0.57 mV/hr, which was 85.46% reduction. Through the back-end calibration circuit to reduce the hysteresis effect, the VH for the forward cycle and reverse cycle of the urea biosensor modified by Au NPs were reduced by 26% and 30%, respectively. The VH for the forward cycle and reverse cycle of

the urea biosensor modified by γ-Fe$_2$O$_3$ NPs were reduced by 23% and 28%, respectively.

REFERENCES

[1] A. A. Ibrahim *et al.*, "Two-dimensional ytterbium oxide nanodisks based biosensor for selective detection of urea," *Biosens. Bioelectron.*, vol. 98, pp. 254–260, Dec. 2017.

[2] R. Rahmanian, S. A. Mozaffari, H. S. Amoli, and M. Abedi, "Development of sensitive impedimetric urea biosensor using DC sputtered nano-ZnO on TiO$_2$ thin film as a novel hierarchical nanostructure transducer," *Sens. Actuat. B, Chem.*, vol. 256, pp. 760–774, Mar. 2018.

[3] H.-H. Deng, G.-L. Hong, F.-L. Lin, A.-L. Liu, X.-H. Xia, and W. Chen, "Colorimetric detection of urea, urease, and urease inhibitor based on the peroxidase-like activity of gold nanoparticles," *Analytica Chimica Acta*, vol. 915, pp. 74–80, Apr. 2016.

[4] F. Roch-Ramel, "An enzymic and fluorophotometric method for estimating urea concentrations in nanoliter specimens," *Anal. Biochem.*, vol. 21, no. 3, pp. 372–381, Dec. 1967.

[5] M. A. Fuertes, J. M. Pérez, and C. Alonso, "Small amounts of urea and guanidine hydrochloride can be detected by a far-UV spectrophotometric method in dialysed protein solutions," *J. Biochem. Biophys. Methods*, vol. 59, no. 3, pp. 209–216, Jun. 2004.

[6] R. Wang, H. Wu, X. Zhou, and L. Chen, "Simultaneous detection of ethyl carbamate and urea in Chinese yellow rice wine by HPLC-FLD," *J. Liquid Chromatogr. Related Technol.*, vol. 37, no. 1, pp. 39–47, Oct. 2014.

[7] M. Tabata and T. Murachi, "A chemiluminometric method for the determination of urea in serum using a three-enzyme bioreactor," *J. Biolum. Chemilum.*, vol. 2, no. 2, pp. 63–67, Apr.–Jun. 1988.

[8] S. Jakhar and C. Pundir, "Preparation, characterization and application of urease nanoparticles for construction of an improved potentiometric urea biosensor," *Biosens. Bioelectron.*, vol. 100, pp. 242–250, Feb. 2018.

[9] T. Ming *et al.*, "Paper-based microfluidic aptasensors," *Biosens. Bioelectron.*, vol. 170, Dec. 2020, Art. no. 112649.

[10] L. Lan, Y. Yao, J. Ping, and Y. Ying, "Ultrathin transition-metal dichalcogenide nanosheet-based colorimetric sensor for sensitive and label-free detection of DNA," *Biosens. Bioelectron.*, vol. 290, pp. 565–572, Jul. 2019.

[11] Y. Han, J. Chen, Z. Li, H. Chen, and H. Qiu, "Recent progress and prospects of alkaline phosphatase biosensor based on fluorescence strategy," *Biosens. Bioelectron.*, vol. 148, Jan. 2020, Art. no. 111811.

[12] X. Liu, Y. Ying, and J. Ping, "Structure, synthesis, and sensing applications of single-walled carbon nanohorns," *Biosens. Bioelectron.*, vol. 167, Nov. 2020, Art. no. 112495.

[13] C. Zhang, J. Ping, and Y. Ying, "Evaluation of trans-resveratrol level in grape wine using laser-induced porous graphene-based electrochemical sensor," *Sci. Total Environ.*, vol. 714, Apr. 2020, Art. no. 136687.

[14] M. Z. H. Khan, M. R. Hasan, S. I. Hossain, M. S. Ahommed, and M. DaizyBai, "Ultrasensitive detection of pathogenic viruses with electrochemical biosensor: State of the art," *Biosens. Bioelectron.*, vol. 166, Oct. 2020, Art. no. 112431.

[15] L. Lan, Y. Yao, J. Ping, and Y. Ying, "Recent advances in nanomaterial-based biosensors for antibiotics detection," *Biosens. Bioelectron.*, vol. 91, pp. 504–514, May 2017.

[16] Y.-H. Nien *et al.*, "Investigation of flexible arrayed urea biosensor based on graphene oxide/nickel oxide films modified by Au nanoparticles," *IEEE Trans. Instrum. Meas.*, vol. 70, Aug. 2020, Art. no. 1500409.

[17] Y.-H. Nien *et al.*, "The analysis of potentiometric flexible arrayed urea biosensor modified by graphene oxide and γ-Fe$_2$O$_3$ nanoparticles," *IEEE Trans. Electron Devices*, vol. 67, no. 11, pp. 5104–5110, Nov. 2020.

[18] G. Maduraiveeran, M. Sasidharan, and V. Ganesan, "Electrochemical sensor and biosensor platforms based on advanced nanomaterials for biological and biomedical applications," *Biosens. Bioelectron.*, vol. 103, pp. 113–129, Apr. 2018.

[19] J.-C. Chou *et al.*, "Characterization of flexible arrayed pH sensor based on nickel oxide films," *IEEE Sensors J.*, vol. 18, no. 2, pp. 605–612, Jan. 2018.

[20] P.-Y. Kuo and Z.-X. Dong, "A new calibration circuit design to reduce drift effect of RuO$_2$ urea biosensors," *Sensors*, vol. 19, no. 20, p. 4558, Oct. 2019.

[21] S.-C. Tseng *et al.*, "Research of non-ideal effect and dynamic measurement of the flexible-arrayed chlorine ion sensor," *IEEE Sensors J.*, vol. 16, no. 12, pp. 4683–4690, Jun. 2016.

[22] J.-C. Chou *et al.*, "Data fusion and fault diagnosis for flexible arrayed pH sensor measurement system based on LabVIEW," *IEEE Sensors J.*, vol. 14, no. 5, pp. 1405–1411, May 2014.

[23] J.-C. Chou, Y.-L. Tsai, T.-Y. Cheng, Y.-H. Liao, G.-C. Ye, and S.-Y. Yang, "Fabrication of arrayed flexible screen-printed glucose biosensor based on microfluidic framework," *IEEE Sensors J.*, vol. 14, no. 1, pp. 178–183, Jan. 2014.

[24] J.-C. Chou *et al.*, "The fabrication and sensing characteristics of arrayed flexible IGZO/Al urea biosensor modified by graphene oxide," *IEEE Trans. Nanotechnol.*, vol. 16, no. 6, pp. 958–964, Nov. 2017.

[25] N. H. Chou, J. C. Chou, T.-P. Sun, and S. K. Hsiung, "Study on the disposable urea biosensors based on PVC-COOH membrane ammonium ion-selective electrodes," *IEEE Sensors J.*, vol. 6, no. 2, pp. 262–268, Apr. 2006.

[26] J.-L. Wang, P.-Y. Yang, T.-Y. Hsieh, C.-C. Hwang, and M.-H. Juang, "pH-sensing characteristics of hydrothermal Al-doped ZnO nanostructures," *J. Nanomater.*, vol. 2013, Oct. 2013, Art. no. 152079.

[27] L. Bousse, H. Van Den Vlekkert, and N. De Rooij, "Hysteresis in Al$_2$O$_3$-gate ISFETs," *Sens. Actuat. B, Chem.*, vol. 2, no. 2, pp. 103–110, May 1990.

[28] A. Das *et al.*, "Highly sensitive palladium oxide thin film extended gate FETs as pH sensor," *Sens. Actuat. B, Chem.*, vol. 205, pp. 199–205, Dec. 2014.

[29] C.-N. Tsai, J.-C. Chou, T.-P. Sun, and S.-K. Hsiung, "Study on the sensing characteristics and hysteresis effect of the tin oxide pH electrode," *Sens. Actuat. B, Chem.*, vol. 108, nos. 1–2, pp. 877–882, Jul. 2005.

JUNG-CHUAN CHOU (Senior Member, IEEE) was born in Tainan, Taiwan, in July 13, 1954. He received the B.S. degree in physics from Kaohsiung Normal College, Kaohsiung, Taiwan, in 1976, the M.S. degree in applied physics from Chung Yuan Christian University, Chung-Li, Taiwan, in 1979, and the Ph.D. degree in electronics from National Chiao Tung University, Hsinchu, Taiwan, in 1988. He taught at Chung Yuan Christian University from 1979 to 1991. Since 1991, he has been an Associate Professor with the Department of Electronic Engineering, a Professor with the Department of Electronic Engineering since 2010, and the Deputy Direct of Headquarter, Testing Center for Technological and Vocational Education, National Yunlin University of Science and Technology, since 2018. From 1997 to 2002, he was the Dean of Office of Technology Cooperation, the Chief Secretary from 2002 to 2009, and the Director of Library from 2009 to 2010, the Office of Research and Development from 2010 to 2011, and the Administration, Testing Center for Technological and Vocational Education, National Yunlin University of Science and Technology, Yunlin, Taiwan, from 2010 to 2011. His research interests are in the areas of sensor material and device, biosensor and system, microelectronic engineering, optoelectronic engineering, solar cell, and solid state electronics. He worked as a Distinguished Professor with the Department of Electronic Engineering, National Yunlin University of Science and Technology, from 2011 to 2017. Since 2018, he has been the Lifetime Chair Professor with the Department of Electronic Engineering, National Yunlin University of Science and Technology.

YU-HSUN NIEN (Member, IEEE) was born in Chunghwa, Taiwan, in 1968. He received the B.S. degree from the Department of Chemistry, National Sun Yat-sen University, Taiwan, the master's degree from the Department of Chemical Engineering, Illinois Institute of Technology, Chicago, IL, USA, and the Ph.D. degree from the Department of Materials Science and Engineering, Drexel University, Philadelphia, PA, USA, in 2000. He is currently a Professor with the Department of Chemical and Materials Engineering, National Yunlin University of Science and Technology, Yunlin, Taiwan. His research focuses on the biomaterials, dye sensitized solar cell, photocatalyst, and applications of nanofibers. His works in nano-fibrous filter systems are awarded by the Taiwan FITI Competition and the National Innovation Award.

PO-YU KUO (Member, IEEE) was born in Taichung, Taiwan, in 1980. He received the M.S. and Ph.D. degrees in electrical engineering from the University of Texas at Dallas in 2006 and 2011, respectively. In 2013, he joined the Department of Electronic Engineering with the National Yunlin University of Science and Technology, Yunlin, Taiwan, where he is currently an Assistant Professor. His research interests include the analog circuits, power management circuits, and analog circuit model analysis.

CHIH-HSIEN LAI (Member, IEEE) was born in Taichung, Taiwan, in 1968. He received the B.S. and M.S. degrees in electrical engineering and the Ph.D. degree in photonics and optoelectronics from National Taiwan University, Taipei, Taiwan, in 1990, 1992, and 2010, respectively. He had worked with the Telecommunications Industry for a number of years. He was an Assistant Professor with the Department of Electronic Engineering, Hwa Hsia Institute of Technology, Taipei, from 2004 to 2012. In 2012, he joined the Department of Electronic Engineering, National Yunlin University of Science and Technology, Yunlin, Taiwan, where he is currently a Professor. His current research interests include the optical and terahertz guided-wave structures, nanophotonic devices, and optoelectronic devices.

TZU-YU SU was born in Kaohsiung, Taiwan, in May 17, 1996. She received the B.S. degree from the Department of Chemical Engineering, I-SHOU University, Kaohsiung, in 2018, and the M.S. degree from the Department of Chemical Engineering and Materials Engineering, National Yunlin University of Science and Technology, Yunlin, Taiwan, in 2020. She has expertise in biosensor application and electrochemical analysis.

CHIH-SUNG HO received the Ph.D. degree from the Department of Materials Science, University of Southern California, Los Angeles, CA, USA, in 2001. He is currently an Assistant Professor, Tunghai University, Taichung, Taiwan. His research is focused on materials science.

ZHE-XIN DONG (Member, IEEE) was born in Yunlin, Taiwan, in September 23, 1994. He received the B.S. degree from the Department of Electronic Engineering from Cheng Shiu University, Kaohsiung City, Taiwan, in 2018, and the M.S. degree from the Department of Electronic Engineering, National Yunlin University of Science and Technology, Yunlin, Taiwan, in 2020. His research interests include analog circuit design and calibration technique for non-ideal effect of biosensors.

TSU-YANG LAI was born in Taoyuan, Taiwan, in January 21, 1996. He received the B.S. degree from the Department of Communication Engineering, I-SHOU University, Kaohsiung, Taiwan, in 2018, and the M.S. degree from the Department of Electronic Engineering, National Yunlin University of Science and Technology, Yunlin, Taiwan, in 2020. He has expertise in biosensor application.

ZHI-XUAN KANG was born in Taipei, Taiwan, in July 9, 1997. He received the bachelor's degree from the Department of Medicinal Chemistry, Chia Nan University of Pharmacy and Science, Tainan, Taiwan, in 2019. He is currently pursuing the master's degree with the Graduate School of Chemical and Materials Engineering, National Yunlin University of Science and Technology. His current research includes biosensor.